ENCIT 2018

ABCM Associação Brasileira de Engenharia e Ciências Mecânicas

17th Brazilian Congress of Thermal Sciences and Engineering
November 25th-28th, 2018, Águas de Lindóia, SP, Brazil

ENCIT-2018-0193
UFRN'S INWARD ACADEMIC SCRAMJET COUPLED TO FTI ROCKET MOTOR TO DEMONSTRATE SUPERSONIC COMBUSTION

Paulo Gilberto de Paula Toro
João Lucas Correia Barbosa de Farias
George Santos Marinho
Jonatha Wallace da Silva Araújo
Universidade Federal do Rio Grande do Norte/UFRN – Centro de Tecnologia. Av. Senador Salgado Filho, 3000 – Campus Universitário, Lagoa Nova CEP 59.078-970 – Natal/RN – Brasil
toro@ct.ufrn.br; fariasjota09@gmail.com; gmarinho@ct.ufrn.br; jonatha_wallace@hotmail.com

Gilvan Luiz Borba
Universidade Federal do Rio Grande do Norte/UFRN – Centro de Ciências Exatas e da Terra. Av. Senador Salgado Filho, 3000 – Campus Universitário, Lagoa Nova, CEP 59.078-970 – Natal, RN – Brasil
gilvan@geofisica.ufrn.br

Israel da Silveira Rêgo
Instituto de Estudos Avançados/IEAv - Trevo Coronel Aviador José Alberto Albano do Amarante, n°1 Putim CEP. 12.228-001 São José dos Campos, SP – Brasil
israel.rego@ieav.ct.br

Abstract. *This paper shows details of the aerothermodynamic conception and the mechanical design of an academic scramjet for flying with speed corresponding to a Mach number of 4.18 and altitude of 6.2 km, which consists in a symmetrical oblique convergent inward-turning inlet ramps followed by the isolator, the combustor and the expansion section engine to operate in high supersonic regime. The Foguete de Treinamento FTI will accelerate the academic scramjet to the flight conditions. The methodology to design the scramjet geometry and calculate the aerothermodynamic proprieties of the airflow along it was the oblique shock wave theory (for the compression section), Rayleigh flow (for the combustion section) and Prandtl-Meyer flow coupled with area ratio relations (for the expansion section). For the mechanical design a CAD software will be used. The possibility of using airbreathing propulsion system based on supersonic combustion to replace the current propulsion systems within the next decades for cheaper, safer and more sustainable access to space has been the main motivation for this research.*

Keywords: *scramjet, supersonic combustion ramjet, hypersonic airbreathing propulsion, thermal analysis*

1. INTRODUCTION

The feasibility of a reliable hypersonic airbreathing engine (scramjet) is being pursued by several research centers around the world. Brazil is one of the few countries in the world investing in Research, Development and Innovation in supersonic combustion (scramjet) technology for aerospace applications.

Several researchers from Universidade Federal do Rio Grande do Norte (UFRN) and from Instituto de Estudos Avançados (IEAv) have joined efforts with the objective to conduct scientific research and technological development related to hypersonic ground testing facilities and to hypersonic airbreathing propulsion system based on supersonic combustion (scramjet) technology.

An inward two-dimensional academic scramjet, composed by symmetrical oblique convergent inward-turning inlet ramps (Fig. 1) followed by the isolator, the combustor and the expansion section, has been designed to be a hydrogen powered scramjet engine on an acceleration mission of 1.319 km/s (corresponding to approximately Mach number 4) at about 6.2 km geometric altitude.

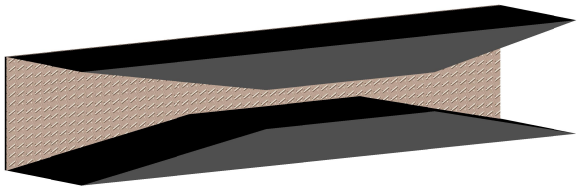

Figure 1: Schematic of the inward-turning scramjet concept.

2. METHODOLOGY

Analytical theoretical analysis, computational fluid dynamics simulation and experimental investigation are the methodologies used to design a technological demonstrator, before flight throughout Earth's atmosphere.

Two-dimensional steady state, non-viscous, no heat conduction compressible flow applied to the shock and expansion waves may be used as analytical theoretical analysis. Also, the 1-D flow with heat addition may be used to simulate the combustion process of the supersonic atmospheric airflow with the fuel at the combustion chamber. Finally, area ratio equations should be used coupled with expansion Prandtl-Meyer theory.

Available commercial CFD codes are able to investigate numerically the turbulent real gas hypersonic airflow under combustion process. Reflected hypersonic shock tunnels are ground-based experimental facilities capable to duplicate the flight conditions.

Nomenclature needed not only in the analytical theoretical analysis but also in the numerical simulation and experimental investigations is presented by Heiser and Pratt (1994) and it is adapted for the inward-turning scramjet, which is divided in three main components (Fig. 2): internal compression section (inlet), combustion chamber (combustor) and internal expansion section (outlet).

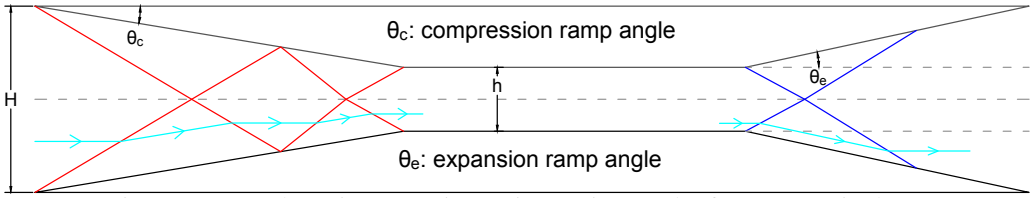

Figure 2: Inward-turning scramjet engine stations and reference terminology.

The goal of this project is to design, based on the analytical theoretical analysis, an inward two-dimensional academic scramjet (Fig. 1) for flight demonstration at about 1.319 km/s and 6.2 km altitude. The cross-section height of the vehicle is 275 mm. The combustor chamber is 500 mm long with constant area. The constant area combustion chamber is 49 mm high (to accommodate the airflow captured by the inward two-dimensional scramjet inlet frontal area). The baseline geometry of the inward 2-D academic scramjet inlet (Fig. 3) is taken as a θ_c leading-edge ramp with 100 mm span.

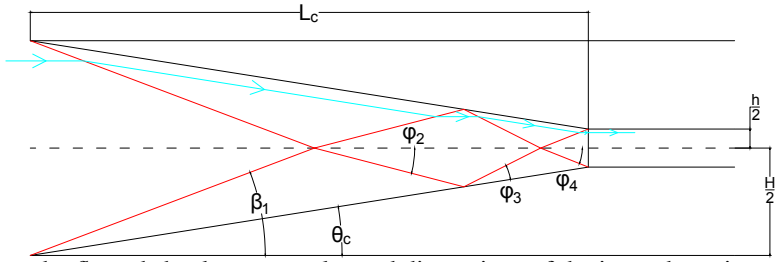

Figure 3: Incident and reflected shock wave angles and dimensions of the inward-turning academic scramjet.

2.1 Shock Wave Theory

Supersonic flow adjusts to the presence of a body through shock waves, causing abrupt changes in fluid properties. When the flow encounters a wedge, an oblique shock wave is formed attached to the body's vertice and inclined at an angle known as the wave angle (β). Flow after the shock is uniform, parallel to the surface of the wedge in such a way that the fluid changed its trajectory according to θ, the angle of deflection (John, 1969). Figure 4 shows a schematic representation of an oblique shock wave.

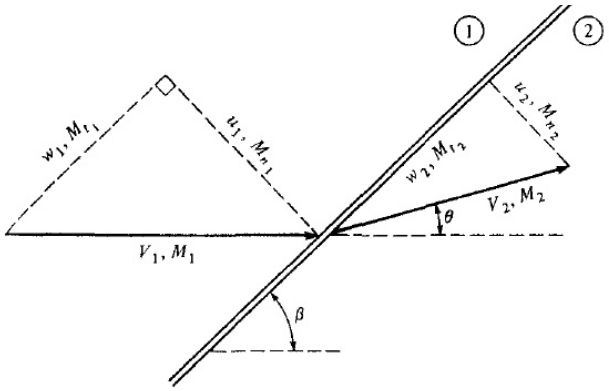

Figure 4: Oblique shock wave. Adapted from (Anderson Jr., 1990).

Considering no boundary-layer effects (non-viscous flow), calorically perfect gas, one-dimensional adiabatic flow and using *Navier-Stokes Equations* it is possible to find equations that relate the aerothermodynamic properties before and after the shock wave. Equation 1 shows the relation between the deflection angle and the wave angle. Using Eqs. 2, 3, 4 and 5 it's possible to caculate the flow properties after the oblique shock wave.

$$tg(\theta) = 2\,cotg(\beta)\left[\frac{M_1^2 sen^2(\beta) - 1}{M_1^2(\gamma + cos(2\beta)) + 2}\right] \tag{1}$$

$$M_{n_2}^2 = \frac{1 + \frac{\gamma - 1}{2} M_{n_1}^2}{\gamma M_{n_1}^2 - \frac{\gamma - 1}{2}} \tag{2}$$

$$\frac{T_2}{T_1} = \left[1 + \frac{2\gamma}{\gamma + 1}(M_{n_1}^2 - 1)\right]\left[\frac{2 + (\gamma - 1)M_{n_1}^2}{M_{n_1}^2(\gamma + 1)}\right] \tag{3}$$

$$\frac{p_2}{p_1} = 1 + \frac{2\gamma}{\gamma + 1}(M_{n_1}^2 - 1) \tag{4}$$

$$\frac{\rho_2}{\rho_1} = \frac{M_{n_1}^2(\gamma + 1)}{[2 + (\gamma - 1)M_{n_1}^2]} \tag{5}$$

When an oblique shock wave encounters a surface or another oblique shock wave, a reflected shock wave is formed. The flow must be parellel to the new surface, therefore the reflection has the same angle of deflection as the incident shock wave (Fig. 5). The same equations used on the incident shock wave can be applied to the reflected shock wave. The incident shock waves and the reflections can be seen as red lines in Fig. 3.

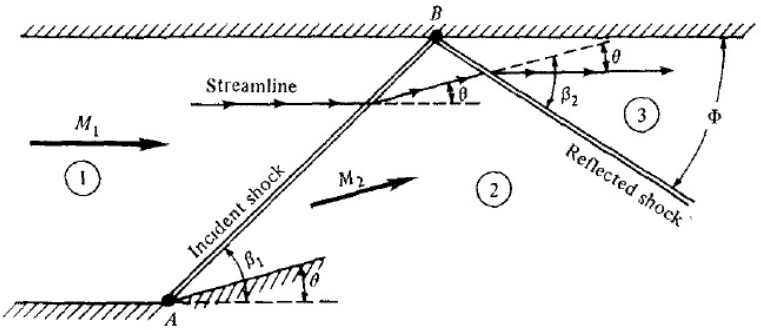

Figure 5: Reflection of an oblique shock wave Anderson Jr. (1990).

2.2 Heat Adittion

The combustion process can be modelled as a heat addition through the system's boundaries. Inviscid, one-dimenional flow with heat addition, known as Rayleigh Flow, may be applied to the combustion process to determine the governing

equations that relate the flow properties before and after the combustion. Equation 6 represents the amount of energy, in $\mathrm{kJ/kg}$, that is added to the system. The Mach number after the combustion is considered to be equal to 1.2. This value is chosen due to the fact that the flow must remain supersonic throughout all the stages of the scramjet. With this value, it is possible to calculate the thermodynamic properties after the heat addition using Eqs. 7, 8, 9 and 10 (Anderson Jr., 1990).

$$q = \left(c_p T_2 + \frac{u_2^2}{2}\right) - \left(c_p T_1 + \frac{u_1^2}{2}\right) = c_p T_{o_2} - c_p T_{o_1} \quad \Rightarrow \quad q = c_p (T_{o_2} - T_{o_1}) \tag{6}$$

$$\frac{T_2}{T_1} = \left(\frac{1+\gamma M_1^2}{1+\gamma M_2^2}\right)^2 \cdot \left(\frac{M_2}{M_1}\right)^2 \tag{7}$$

$$\frac{P_2}{P_1} = \frac{1+\gamma M_1^2}{1+\gamma M_2^2} \tag{8}$$

$$\frac{\rho_2}{\rho_1} = \left(\frac{1+\gamma M_2^2}{1+\gamma M_1^2}\right) \cdot \left(\frac{M_1}{M_2}\right)^2 \tag{9}$$

$$\frac{T_{o_2}}{T_{o_1}} = \left(\frac{1+\gamma M_1^2}{1+\gamma M_2^2}\right)^2 \cdot \left(\frac{M_2}{M_1}\right)^2 \cdot \left(\frac{1+\frac{\gamma-1}{2} M_2^2}{1+\frac{\gamma-1}{2} M_1^2}\right) \tag{10}$$

2.3 Expansion Wave Theory

When supersonic flow goes over a convex corner, the fluid adjusts to the surface through an expansion wave as shown in Fig. 6. This process is known as Prandtl-Meyer flow. The process happens through a series of gradual, reversible expansions gerenating Mach waves that spread out (John, 1969). The flow is adiabatic and reversible and, therefore, is isentropic. Thus, it's possible to use the isentropic relations to calculate the changes in thermodynamic properties.

Equation 12 shows the relation between the expansion angle (θ) and the Mach number before and after the process. With the function $\nu(M)$ (Eq. 11) it is possible to calculate the Mach number after the expansion and, using the isentropic relations, the closed form of the thermodynamic properties (static pressure, static density and static temperature) ratios across the expansion wave can be determined.

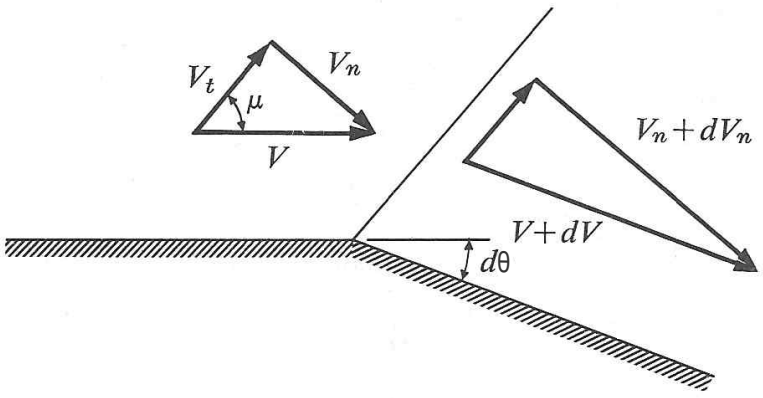

Figure 6: Supersonic flow over convex corner forming an expansion wave.

$$\nu(M) = \sqrt{\frac{\gamma+1}{\gamma-1}} \cdot tg^{-1}\left(\sqrt{\frac{\gamma-1}{\gamma+1}(M^2-1)}\right) - tg^{-1}\left(\sqrt{M^2-1}\right) \tag{11}$$

$$\theta = \nu(M_2) - \nu(M_1) \tag{12}$$

$$\frac{T_2}{T_1} = \frac{1+\frac{\gamma-1}{2}M_1^2}{1+\frac{\gamma-1}{2}M_2^2} \tag{13}$$

$$\frac{P_2}{P_1} = \left(\frac{1+\frac{\gamma-1}{2}M_1^2}{1+\frac{\gamma-1}{2}M_2^2}\right)^{\frac{\gamma}{\gamma-1}} \tag{14}$$

$$\frac{\rho_2}{\rho_1} = \left(\frac{1+\frac{\gamma-1}{2}M_1^2}{1+\frac{\gamma-1}{2}M_2^2}\right)^{\frac{1}{\gamma-1}} \tag{15}$$

When an expansion wave encounters a surface or another expansion wave, a reflected expansion wave is formed. For simplification, it is considered that the Mach angle (μ) ahead of the reflected wave is equal to the Mach angle ahead of the incident wave. The same equations used on the expansion wave can be applied to the reflected expansion wave. The incident expansion waves and the reflections can be seen as blue lines in Fig. 7.

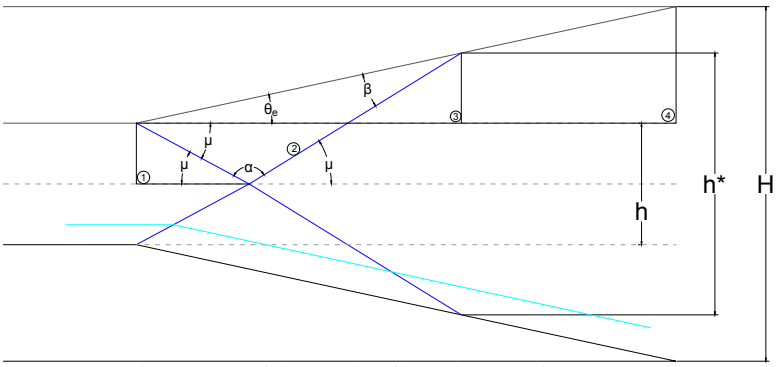

Figure 7: Incident and reflected expansion waves.

2.4 Area Ratio

When supersonic flow goes through a nozzle, the Mach number and the thermodynamic properties of the fluid tend to change according to how the area of the nozzle changes. Area ratio equations are valid for isentropic flow and relate the ratio of Mach number at two points of the nozzle to the ratio of the nozzle area at those two points (Eq. 16). By knowing the area ratio it is possible to compute the Mach number at the end of the process and, using the isentropic relations, calculate the changes in thermodynamic properties (Eqs 17, 18 and 19).

$$\left(\frac{A_2}{A_1}\right)^2 = \left(\frac{M_1}{M_2}\right)^2 \left(\frac{1+\frac{\gamma-1}{2}M_2^2}{1+\frac{\gamma-1}{2}M_1^2}\right)^{\frac{\gamma+1}{\gamma-1}} \tag{16}$$

$$\frac{T_2}{T_1} = \frac{1+\frac{\gamma-1}{2}M_1^2}{1+\frac{\gamma-1}{2}M_2^2} \tag{17}$$

$$\frac{P_2}{P_1} = \left(\frac{1+\frac{\gamma-1}{2}M_1^2}{1+\frac{\gamma-1}{2}M_2^2}\right)^{\frac{\gamma}{\gamma-1}} \tag{18}$$

$$\frac{\rho_2}{\rho_1} = \left(\frac{1+\frac{\gamma-1}{2}M_1^2}{1+\frac{\gamma-1}{2}M_2^2}\right)^{\frac{1}{\gamma-1}} \tag{19}$$

3. RESULTS AND COMMENTARIES

On Tab. 1 it is shown some properties of fuels usually used on the study of atmospheric air mixture combustion. It is possible to notice that hydrogen gas has higher values of auto-ignition temperature and heating value than any other hydrocarbon listed.

Table 1: Properties of fuels used in aerospace applications.

Fuel	Formula	Auto-ignition temperature (K)	Heating value h_{pr} (MJ/kg)
Hydrogen	H_2	845,15	119,954
Methane	CH_4	810,15	50,010
Ethane	C_2H_6	745,15	47,484
Hexane	C_6H_{14}	498,15	45,100
Octane	C_8H_{18}	479,15	44,786
JP-7	$C_{12}H_{25}$	514,15	43,903
JP-10	$C_{10}H_{16}$	518,15	42,100

Heiser and Pratt (1994) e Coordinating Research Council (1983).

The thermodynamic properties at the inward-turning scramjet engine baseline (Fig. 3) may be determined based on the two-dimensional compressible flow (oblique shock wave relationships) considering the simplest case, i. e., inviscid flow, calorically perfect air gas and scramjet engine with power on (Tab. 1). Three cases were studied: the first with 9° leading-edge deflection angle, the second with 11° and the third with 13°. It was applied the following restriction: there are incident shock waves generated due to the alignment of the leading-edge with the undisturbed freestream air flow; the last reflected shock waves generated at symmetric center line hit the entrance of the combustor chamber, where the flow will enter with constant static pressure, constant static temperature, constant static density and constant supersonic airflow. Then, fuel (H_2) and air burn together in order to provide heat addition to the flow. At the end of the combustion chamber, airflow is still supersonic with Mach number equal to 1.2 for all cases studied.

After the combustor, air and fuel mixture goes through an expansion with 25° deflection angle and a reflection of the expansion wave generated. Then, no more expansion waves take place and the flow through the exit nozzle itself is responsible for expanding and accelerating the mixture, since it is a divergent nozzle with flow at supersonic speed. These changes are accounted for using area ratio equations. Finally, the mixture leaves the scramjet body and encounters the FTI body at which another oblique shock wave is generated. Only then, the flow leaves the ensemble and its final proprieties are calculated so as to check if there's thrust generation.

The changes in Mach number, scramjet velocity, temperature and pressure along the vehicle stages can be seen in Figs. 9, 10 and 11. The first values shown represent the freestream proprieties and the last ones represent the proprieties after the flow leaves the scramjet-FTI ensemble. After the flow is expanded, it goes through another oblique shock (with 15° deflection angle) due to the presence of the FTI, only then it leaves the ensemble (Fig. 8).

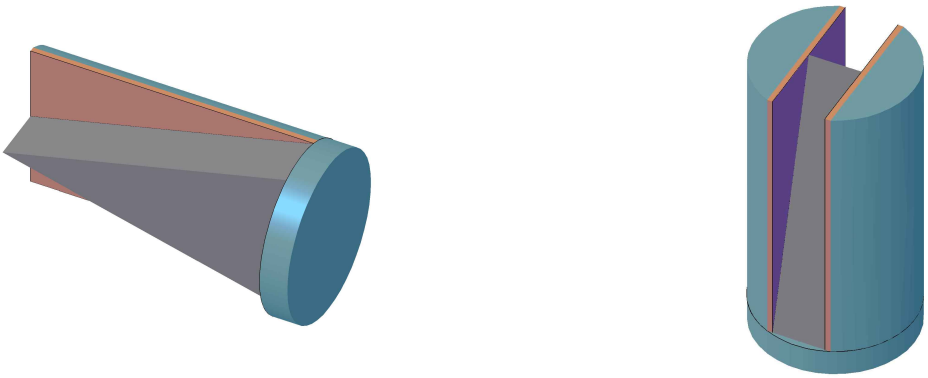

(a) Partial 3D view of the scramjet-FTI ensemble. (b) Complete 3D view of the scramjet-FTI ensemble

Figure 8: Superior edge of the FTI where the scramjet is placed.

Table 2 shows the aerothermodynamic flight conditions for the scramjet studied. The values of altitude and Mach number were obtained from the flight conditions of the FTI itself whereas the other values were obtained from US Standard Atmosphere (1976) for the given altitude.

Table 2: Flight conditions.

Altitude (km)	M	T (K)	P (Pa)	ρ (kg/m^3)	R (J/kg K)
6,2125	4,18	247,8	45860	0,6447	287

FTI trajectory and US Standard Atmosphere (1976).

The body of the scramjet on each figure is divided in different sections so as to better represent the changes in proprieties. Before section A is the freestream flow. The section A-B represents the first part of the compression process and section B-C the second part of the compression process. Section C-D describes the isolator which represents the flow after it's fully compressed and before the combustion process begins that is represented by the section D-E. Section E-D represents the expansion processes: the expansion wave and its reflection. The expansion caused by the area variance at the exit nozzle (area ratio) is represented in section F-G. Finally, the outlet shock caused by the presence of the FTI is represented after section G.

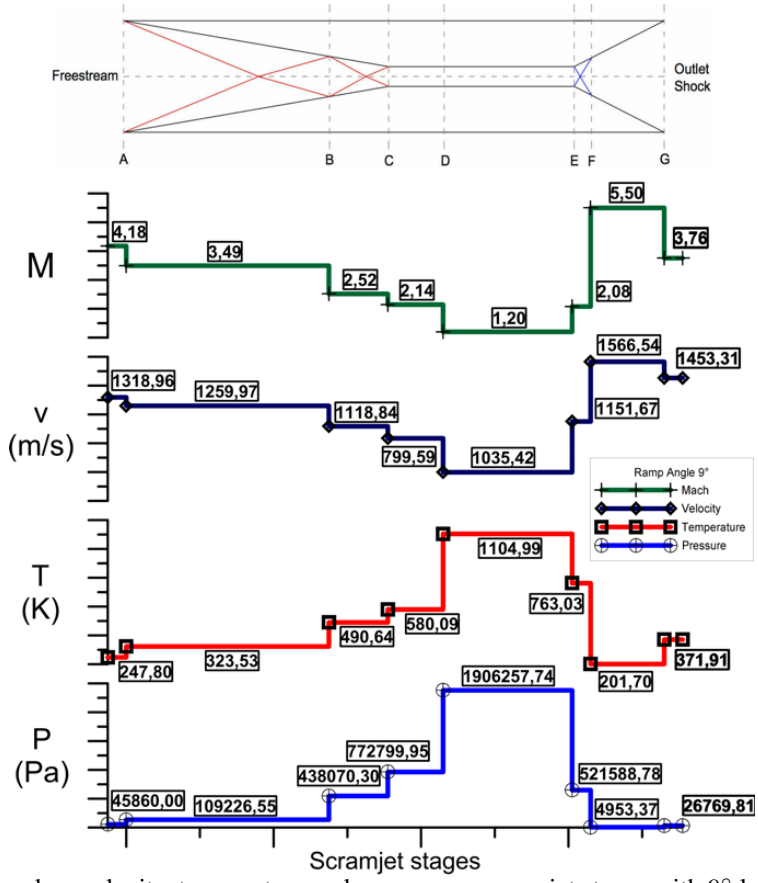

Figure 9: Mach number, velocity, temperature and pressure on scramjet stages with 9° leading-edge angle.

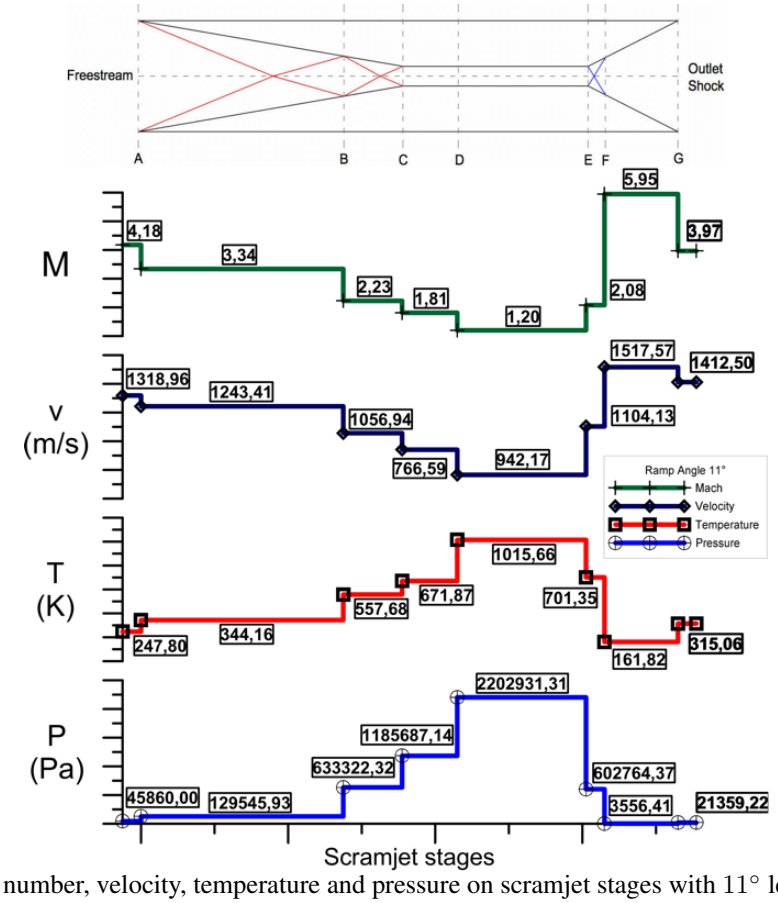

Figure 10: Mach number, velocity, temperature and pressure on scramjet stages with 11° leading-edge angle.

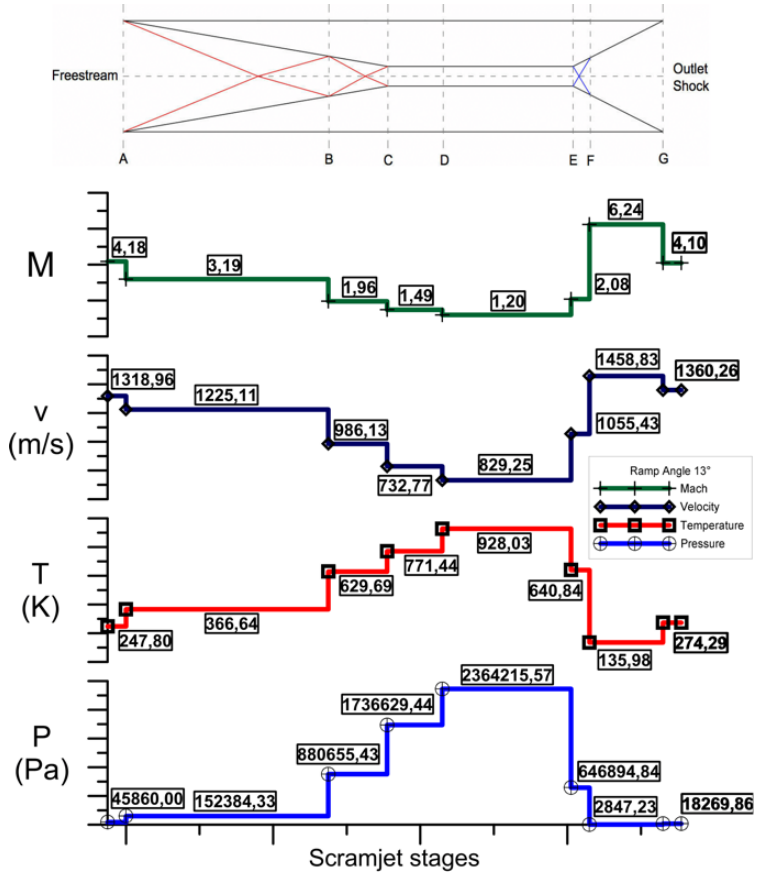

Figure 11: Mach number, velocity, temperature and pressure on scramjet stages with 13° leading-edge angle.

The most relevant values of the graphs for analyzing are the Mach number, temperature and speed at the entrance of the combustion chamber; the Mach number, temperature and pressure at the exit of the combustion chamber and the speed of the air-fuel mixture after the outlet shock. The Mach number at the entrance of the combustor must be supersonic and high enough to remain supersonic after the head addition. The temperature must be high enough to auto ignite the fuel (H_2). The airflow speed is taken into account when calculating the length of the combustor in order to assure combustion occurs properly.

The Mach number at the exit of the combustor is always equal to 1.2, a restriction implemented to make sure the flow remains supersonic. After the outlet shock caused by the presence of the FTI, the flow speed must be higher than the freestream airflow speed in order to provide thrust to the vehicle.

As expected, the higher the value of the leading-edge angle the lesser the value of the Mach number at the entrance of the combustor. Consequently, the temperature at the entrance of the combustor is higher with higher leading-edge angle. In all three cases analyzed, the Mach number remains supersonic and the temperature is lower than the auto-ignition temperature of the hydrogen gas. Due to that fact, an ignitor is needed in order for the combustion to happen. Also, for all values of leading-edge angles analyzed the exit velocity is higher than the freestream velocity, that is, for all cases there's thrust generation.

The goal of the graphs shown in Figs. 9, 10 and 11 is to better illustrate how the aerothermodynamics proprieties change along the scramjet sections. One of the most important things to notice is the difference in intensity of the expansions processes. The Mach number increases way more during the the area ratio process than it does during Prandtl-Meyer expansion and reflection. Also, temperature decreases more during area ratio process. Finally, the pressure decreases more during Prandtl-Meyer expansion but only in absolute value. In relative value, the pressure follows the same logic as the temperature: the decrease is greater during area ratio process.

4. CONCLUSION AND OUTLOOK FOR FUTURE PROJECTS

Calculations were performed by varying the scramjet geometry, in the compression section and assessed the implications of this in order to select the best configuration for the mechanical design of the scramjet. In conclusion, the three different scramjet geometries analyzed are capable of generating thrust. Although they add different amounts of heat to the system, they all maintain supersonic flow during the whole process and neither of them reach the temperature needed for auto-ignition of H_2. Thus, an ignitor must be used in order to start the combustion process. Finally, the calculations

show that supersonic combustion using scramjet technology is theoretically possible.

5. ACKNOWLEDGEMENTS

The first five authors would like to thank Universidade Federal do Rio Grande do Norte (UFRN) for the support given to complete this scientific work. The first author (as Visiting Professor) would like to express appreciation to UFRN for the possibility of applying the knowledge in aerothermodynamics and hypersonics in the research area in hypersonic airbreathing propulsion based on supersonic combustion ramjet (scramjet) technology. A portion of this effort was supported by Instituto de Estudos Avançados (IEAv) and by the Propulsão Hipersônica 14-X (PropHiper) Project and the last author would like to express his appreciation.

6. REFERENCES

Anderson Jr., J.D., 1990. *Modern Compressible Flow*. McGraw-Hill, New York, 2nd edition.

Coordinating Research Council, 1983. *Handbook of Aviation Fuel Properties*. Coordinating Research Council, Atlanta.

Heiser, W.H. and Pratt, D.T., 1994. *Hypersonic Airbreathing Propulsion*. American Institute of Aeronautics and Astronautics, Washington.

John, J.E.A., 1969. *Gas Dynamics*. Ally and Bacon, Pearson Education, Boston.

US Standard Atmosphere, 1976. *US Standard Atmosphere*. National Oceanic and Atmospheric Administration, Washington.

7. RESPONSIBILITY NOTICE

The following text, properly adapted to the number of authors, must be included in the last section of the paper:
The author are the only responsible for the printed material included in this paper.
The authors declare that there is no conflict of interest regarding the publication of this scientific article.